Aluminium siting in the ZSM-5 framework by combination of high resolution ^{27}Al NMR and DFT/MM calculations†

Stepan Sklenak,*[a] Jiří Dědeček,[a] Chengbin Li,[a] Blanka Wichterlová,[a] Vendula Gábová,[a] Marek Sierka[b] and Joachim Sauer[b]

Received 7th May 2008, Accepted 29th September 2008
First published as an Advance Article on the web 12th December 2008
DOI: 10.1039/b807755j

The Al siting in the ZSM-5 zeolite was investigated by ^{27}Al 3Q MAS NMR spectroscopy and QM/MM calculations. It was found that the occupation of the framework T-sites by Al and the concentration of Al in these T-sites are neither random nor controlled by a simple rule. They both depend on the conditions of the zeolite synthesis. At least 12 out of the 24 distinguishable framework T-sites of ZSM-5 are occupied by Al in the set of the investigated zeolite samples. A partial identification of the Al sites is possible. The calculated ^{27}Al NMR shielding values were converted to ^{27}Al isotropic chemical shifts using the experimental isotropic chemical shift of 60.0 ppm referenced to the aqueous solution of $Al(NO_3)_3$ and the corresponding calculated NMR shielding of 490.0 ppm of a silicon rich (Si/Al 38) chabazite structure zeolite as a secondary internal standard. The observed ^{27}Al isotropic chemical shifts of 50.0 and 54.7 ppm correspond to Al atoms in the T20 and T6 sites, respectively. The pair of measured isotropic chemical shifts of 52.9 and 53.7 ppm can be assigned to the T4, T8 pair. At the low-shielding end, two assignments are plausible. The smallest deviations between the calculated and observed isotropic chemical shifts are reached for the assignment as follows: T24 (64.8 ppm) is not occupied in the samples and that the observed isotropic chemical shifts 63.6, 62.8, and 60.0 ppm belong to T1, T17, and T7, respectively. It follows then that T-sites T12 (60.8 ppm), T3 (61.7 ppm), and T18 (62.0 ppm) are most likely not occupied by Al in our ZSM-5 samples. If we assume that the calculated isotropic chemical shifts are systematically larger than the observed ones then we can assign the largest observed isotropic chemical shifts of 63.6 and 62.8 ppm to the least shielded T24 and T1 sites, respectively, and 60.0 ppm to T12. Then the sites T3 (61.7 ppm), T18 (62.0 ppm), and T17 (62.5 ppm) would be unoccupied by Al in our ZSM-5 samples. It was further shown that there is no simple linear relationship between the observed ^{27}Al isotropic chemical shifts and the average Al–O–Si angles.

1. Introduction

Zeolites are crystalline microporous aluminosilicates widely used as molecular sieves and catalysts in industrial chemical processes. In the past thirty years, attention was drawn to ZSM-5 and other silicon-rich zeolites (with Si/Al > 12). Their protonic forms are currently used as acid catalysts for hydrocarbon transformations in petrochemistry.[1–4] Their transition metal exchanged forms have been discovered as exceptional redox catalysts for nitrogen oxide abatement,[5,6] and a selective oxidation of hydrocarbons by nitrous oxide.[7]

The species assumed to be the active sites in the mentioned reactions, *i.e.* protons, metal ions and metal-oxo species, are positively charged and compensate the negatively charged aluminosilicate framework. Therefore the Al siting in zeolite frameworks governs the location of the active sites as well as their properties. This is important for both the acid catalyzed hydrocarbon syntheses[8] as well as redox reactions.[9,10] Thus, Al siting in zeolites is of crucial importance for their catalytic behavior.

A typical feature of many silicon-rich zeolites is a high number of crystallographically distinguishable tetrahedral framework sites (T-sites, T = Si or Al) resulting in a high variability of the Al siting. The very first attempts to shed light on the Al siting in silicon-rich zeolites were based on theoretical calculations of the energies of Al atoms in the distinguishable T-sites of these materials.[11–16] The calculated energy differences between structures with Al in different T-sites were small[11,14,15] if the substituted structures were fully relaxed

---

[a] *J. Heyrovský Institute of Physical Chemistry of the Academy of Sciences of the Czech Republic, v.v.i., Dolejškova 3, 182 23 Prague, Czech Republic. E-mail: stepan.sklenak@jh-inst.cas.cz*
[b] *Institut für Chemie, Humboldt-Universität zu Berlin, Unter den Linden, 6, 10099 Berlin, Germany*

† Electronic supplementary information (ESI) available: Structure directing agent and aluminium, silicon and sodium sources used for the synthesis of zeolites (Table S1); force field relative energies of Al in the T-sites of ZSM-5 (Table S2); Al–O–Si angles for the T-sites of ZSM-5 (Table S3); 2D plot of the ^{27}Al 3Q MAS NMR sheared spectrum of Na-ZSM-5/A-Na-ZSM-5/G and Na-ZSM-5/I-Na-ZSM-5/R, F1 and F2 projections of the spectrum and selected normalized slices and projection and slice simulations (Fig. S1); simulations of ^{27}Al single pulse spectra of Na-ZSM-5 zeolites and corresponding individual Gaussian lines (Fig. S2); the complete list of authors for ref. 70; The Cartesian coordinates with T-site designations of the most stable structure of chabazite (Si/Al 47) optimized at QM-Pot. See DOI: 10.1039/b807755j

leading to the conclusion that Al siting is either largely random or kinetically controlled during synthesis. Larger energy differences repeatedly reported in quantum mechanical cluster studies for ZSM-5 are an artifact of geometrically constraint cluster models with fixed atoms at their boundaries.[12,13,16] Diffraction techniques cannot distinguish between Al and Si atoms and thus do not allow direct identification of the Al siting in zeolites. However, Olson *et al.* studied the Cs^+ siting in extraframework positions of ZSM-5 by X-ray diffraction and concluded that the three observed Cs^+ sites indicate a nonrandom Al siting.[17]

^{27}Al solid state NMR spectroscopy was found to be a powerful tool for analyzing the coordination of Al atoms in zeolites,[18–20] and moreover, recent developments of multiple quantum NMR experiments[21] opened new possibilities for studying the structure of AlO_4 in zeolite frameworks. Sarv *et al.*[22] applied this approach to ZSM-5 and found three different tetrahedral Al coordinations. Investigations of the effect of Al concentration in the framework on the ^{27}Al (MQ) MAS NMR spectra of ZSM-5[23] and zeolite Beta[24] indicated a non-random Al siting in these matrices.

Key to the identification of the Al siting in high silica zeolites is assigning the observed ^{27}Al resonances to individual framework T-sites. A linear correlation between the ^{27}Al NMR isotropic chemical shift, δ(Al), and the average T–O–T angle, θ, of the zeolite framework was suggested by Lippmaa *et al.*[25] making reference to the correlation between the ^{29}Si NMR chemical shift and the average Si–O–Si angle for which a semiempirical quantum mechanical rationalization exists.[26] Problems arise from the inability of X-ray crystallography to distinguish between Al and Si atoms. The crystallographic T–O–T angles used in the correlation corresponded to the average values of the Al–O–Si and Si–O–Si angles for the same T-sites (only partly occupied by Al) and do not correspond to the local geometry of AlO_4 tetrahedra. Note that experimental studies employing this correlation did not succeed in deriving the Al siting from the measured NMR parameters.[22–24,27–29] Therefore another approach relating measured NMR parameters to individual T-sites is needed.

Developments in computational chemistry have allowed calculating reasonable zeolite structures as well as NMR parameters. Employing the GIAO-CPHF method[30] Sauer *et al.*[31] calculated the ^{29}Si NMR chemical shifts of all-silica zeolite structures in good agreement with observed chemical shifts (standard deviation of 2.8 ppm). For structures calculated with *ab initio* parametrized force fields[32] the agreement was slightly better than for X-ray structures. For the orthorhombic structure of ZSM-5, the calculations reproduced the correct order of all 12 observed ^{29}Si-NMR signals. Bull *et al.*[33,34] used the GIAO method for calculating the ^{17}O isotropic chemical shifts and the electric field gradients of oxygen in siliceous faujasite and ferrierite. For faujasite a complete assignment of the four observed lines was possible, while for ferrierite only a partial assignment could be achieved. Periodic DFT calculations brought some improvement,[35] but did not change the sequence of signals for the different positions.[36] Kučera and Nachtigall[37] studied the MCM-58 zeolite by periodic DFT. They found that the ^{27}Al NMR isotropic chemical shift of Al in the framework dramatically varies with the coordination of the counter cation in the cationic site and with the number of water molecules coordinated to the counter cation.

In this paper, the distribution of Al atoms over the individual T-sites of the ZSM-5 framework is examined.[38] We found that a bare charged framework represents a realistic model for our calculations of the local geometry of AlO_4 tetrahedra in fully hydrated, cation-containing silicon-rich zeolites.[38] The predictions of the ^{27}Al isotropic chemical shifts corresponding to Al in the individual T-sites are based on calculations of the local structure around the Al-site using a quantum mechanics–molecular mechanics hybrid approach (QM-Pot).[38–40] The subsequent evaluation of the NMR shielding values uses the GIAO method.[30] Both steps are based on the density functional theory (DFT). The calculated Al shieldings were converted to Al isotropic chemical shifts employing the experimental and theoretical NMR parameters obtained for the silicon-rich structure of chabasite.[38]

The predicted isotropic chemical shifts are compared with the results of ^{27}Al 3Q MAS NMR measurements for a set of ZSM-5 samples synthesized under different conditions. Good agreement between calculated and measured ^{27}Al isotropic chemical shifts is found and a partial assignment of observed resonances to specific crystallographic sites in ZSM-5 is made. Moreover, our combined computational and experimental study shows that the Al siting in ZSM-5 is not random and can be substantially varied by the conditions of zeolite syntheses.

2. Experimental methods and samples

A set of samples (A-R) of the ZSM-5 zeolite with Si/Al ratios in the range from 14 to 140, with no Al–O–Si–O–Al sequences and a low concentration of Al–O–$(Si–O)_2$–Al sequences (see section 3.1) was prepared under hydrothermal conditions and autogenous pressure at a temperature of 170 °C with agitation for a period of 7–10 d. The aluminium, silicon and sodium sources and the structure directing agents (SDA) used for synthesis are given in Table S1 of the ESI.† Na-ZSM-5/B and Na-ZSM-5/N were purchased from Conteca B.V. Sweden, Na-ZSM-5/H was provided by the Institute of Oil and Hydrocarbon Gases, Slovnaft and ZSM-5/K by the Research Institute of Inorganic Chemistry Inc., Unipetrol. Na-ZSM-5/M was purchased from Süd-Chemie AG München, Germany. Calcined samples were equilibrated with 0.5 M NaCl to obtain Na-ZSM-5. Ion exchange of zeolites with 0.5 M LiCl was employed to prepare Li-ZSM-5/A and Li-ZSM-5/E from Na-ZSM-5. Na-ZSM-5/E and Na-ZSM-5/H were ion exchanged with 1.0 M NH_4NO_3 and subsequent calcination in an oxygen stream resulted in H-ZSM-5/E and H-ZSM-5/H. An equilibration of the Na-zeolites with 0.05 M $Co(NO_3)_2$ at ambient temperature led to the maximum $[Co^{2+}(H_2O)_6]^{2+}$ loaded zeolites. The synthesis of silicon rich chabazite (Si/Al 38) is described in detail in ref. 41. XRD, KBr-FTIR and SEM indicated good crystallinity of calcined ion exchanged samples. Moreover, FTIR characterization of acid sites *via* adsorption of d_3-acetonitrile as well as ^{29}Si MAS NMR indicated a negligible amount of extraframework Al atoms. The chemical composition of the Na-, Li- and H-ZSM-5 zeolites was determined by using atomic absorption spectrometry and is given together with the maximum $[Co^{2+}(H_2O)_6]^{2+}$ exchange capacity of zeolites in Table 1. ^{29}Si and ^{27}Al MAS NMR and ^{27}Al 3Q MAS NMR experiments were carried out on a Bruker Avance 500 MHz (11.7 T) Wide Bore spectrometer using 4 mm o.d. ZrO_2 rotors with a rotation speed of 5 kHz in the case of ^{29}Si MAS NMR and 12 kHz for ^{27}Al MAS NMR. All the Na- and Li-samples were dried only at ambient temperature to guarantee their full hydration. H-ZSM-5 zeolites were after deamonization at 450 °C washed on a filter and then dried at ambient temperature. A ^{29}Si MAS NMR high-power decoupling experiment with the $\pi/6$ (1.7 μs) excitation pulse and the relaxation delay of 30 s was applied to collect a single pulse spectrum. The chemical shifts were referenced to Q8M8. The framework aluminium content (Si/Al_{FR}) was estimated from the ^{29}Si NMR data.

To allow a quantitative evolution of the ^{27}Al MAS NMR spectra, high-power decoupling pulse sequences with $\pi/12$ (0.7 μs) excitation pulse were applied. The isotropic chemical shifts were referenced to the aqueous solution of $Al(NO_3)_3$. Two-dimensional multi-quantum experiments (2D 3Q) were used to determine the ^{27}Al isotropic chemical shift-δ_{iso} ^{27}Al. The 3Q experiments were performed using the two-pulse z-filtered procedure. A π pulse was used for the excitation and a $\pi/3$ pulse for the conversion. The pulses were individually optimised for each sample. The 2D contour plots presented in the paper are results of a 2D Fourier transformation followed by a shearing transformation. The isotropic chemical shift was estimated using

$$\delta_{iso} = (17\delta_{F1} + 10\delta_{F2})/27$$

where δ_{F1} is the chemical shift in the isotropic and δ_{F2} in the observed dimension. The ^{27}Al 3Q MAS NMR spectroscopy of silicon-rich zeolites is discussed by van Bokhoven[24] and the 3Q MAS NMR technique is explained in detail by Alemany.[21] The ^{29}Si and ^{27}Al MAS NMR spectra, the F1 and F2 projections and the F1 slices of the ^{27}Al 3Q MAS NMR spectra were simulated using the Origin software (Microcall Inc., USA).

Table 1 Chemical composition of the Na-ZSM-5 samples, framework Si/Al ratio (Si/Al_{FR}) estimated from ^{29}Si MAS NMR spectra and the maximum exchange capacity of the samples for $[Co^{2+}(H_2O)_6]^{2+}$ complex (Co_{MAX}/Al)

Zeolite	Si/Al	Na/Al	Si/Al_{FR}	Co_{MAX}/Al
Na-ZSM-5/A	14.5	0.95	15	0.04
Li-ZSM-5/A[b]	14.5	0.05	—	—
Na-ZSM-5/B	44.0	0.99	45	0.07
Na-ZSM-5/C	34.0	1.02	35	0.06
Na-ZSM-5/D	26.0	0.90	25[a]	0.13
Na-ZSM-5/E	15.0	1.01	15	0.12
Li-ZSM-5/E[c]	15.2	<0.02	—	—
H-ZSM-5/E	15.0	<0.02	15	—
Na-ZSM-5/F	26.0	0.84	25[a]	0.15
Na-ZSM-5/G	15.1	0.77	15	0.02
Na-ZSM-5/H	22.5	1.02	25	0.12
H-ZSM-5/H	22.5	<0.02	25	—
Na-ZSM-5/I	34.0	0.98	35	0.01
Na-ZSM-5/J	25.0	0.92	26	0.03
Na-ZSM-5/K	13.8	0.98	14	0.11
Na-ZSM-5/L	28.6	0.99	30	0.03
Na-ZSM-5/M[d]	120	1.0	—	—
Na-ZSM-5/N[d]	140	1.0	—	—
Na-ZSM-5/O	28.7	0.85	30	0.05
Na-ZSM-5/P	20.6	0.85	25	0.05
Na-ZSM-5/Q	34.8	0.90	35	0.13
Na-ZSM-5/R	22.7	0.97	25	0.08

[a] The slightly lower Si/Al_{FR} value compared to Si/Al indicates the limited accuracy of the NMR estimate. [b] Li/Al = 0.95. [c] Li/Al = 0.97. [d] Si/Al_{FR} and Co_{MAX}/Al were not determined due to the low Al concentration.

3. Experimental results

3.1 Al local density and characterization of investigated materials

A typical ^{29}Si MAS NMR spectrum of hydrated Na-zeolite (ZSM-5/F) and its simulation is shown in Fig. 1. It is similar to those reported previously for ZSM-5 zeolites.[42,43] Thus, the resonances above −110 ppm were assigned to Si(4Si) sites. The bands between −103 and −108 ppm correspond to Si(3Si,1Al) sites, *i.e.* Si atoms with one neighboring Al atom. The resonances with chemical shifts below −100 ppm representing Si(2Si,2Al) sites with two Al neighbors were not observed. The spectra of other investigated samples were similar, also without any bands corresponding to Si(2Si,2Al) atoms. This is evidence that Al–O–Si–O–Al sequences are absent in the investigated samples.

The silicon to framework aluminium ratio (see Table 1) of the samples (Si/Al_{FR}) was estimated using[44]

$$Si/Al_{FR} = I/0.25\ I_1$$

where I denotes the total intensity of the ^{29}Si NMR signal in the single pulse experiment and I_1 denotes the intensity of the NMR line corresponding to the Si(3Si,1Al) atoms. This value of Si/Al_{FR} corresponds well to the Si/Al values obtained from the chemical analysis revealing that extra framework Al atoms are not present in the investigated samples.

Table 1 shows the maximum ion exchange capacity of zeolites for divalent $[Co^{2+}(H_2O)_6]^{2+}$ complexes. The exclusive presence of the $[Co^{2+}(H_2O)_6]^{2+}$ complexes in our samples was checked by visible spectroscopy (not shown in the figures).

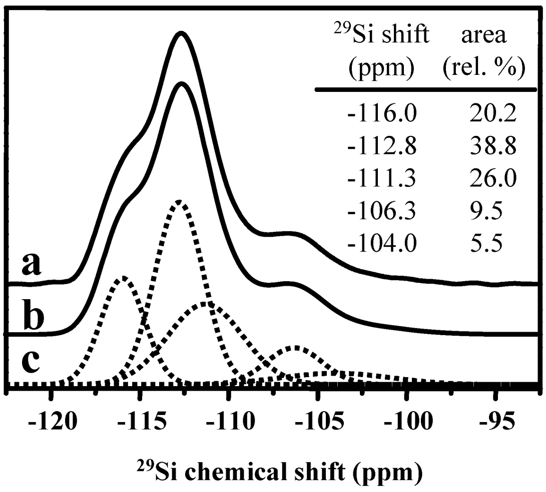

Fig. 1 ^{29}Si MAS NMR spectrum of Na-ZSM-5/F. Experimental data (a), fit (b), Gaussian bands corresponding to the individual resonances (c) and relative areas corresponding to the individual resonances.

The low ion exchange capacity of the ZSM-5 zeolites for divalent complexes indicates that the concentration of close Al atoms in the framework is low (6–30% of Al atoms). The details of the determination of the Al local density by Co^{2+} ions as a probe are discussed elsewhere.[45,46]

3.2 ^{27}Al NMR spectra and Al distribution

All the investigated samples exhibit exclusively the signal centered around 55 ppm in the SP (single pulse) ^{27}Al MAS NMR spectrum (not shown in the figures). This signal corresponds to the Al atoms with a tetrahedral coordination.[25] The resonance around 0 ppm corresponding to octahedrally coordinated Al atoms was not observed in the spectrum confirming the conclusion of the exclusive presence of Al atoms in the zeolite framework based on the ^{29}Si MAS NMR experiment (see above). The 3Q ^{27}Al MAS NMR method was employed to resolve the individual resonances corresponding to different tetrahedrally coordinated Al atoms. A typical 2D plot of the results for Na-ZSM-5 is shown in Fig. 2 and S1 of the ESI† together with the F1 (along the *y* axis) and F2 projections as well as with selected F1 and F2 slices. The F1 and F2 projections of all the samples and their simulations are depicted in Fig. 3 and 2 and Fig. S1 of the ESI.† The NMR parameters (Tables 2 and 3)—the δ_{F1} and δ_{F2} values and the Al isotropic chemical shifts (δ_{iso}) were obtained from a simulation of the F1 and F2 projections and F1 and F2 slices. Note that the same Al isotropic chemical shift can correspond to different resonances differing in their δ_{F1} and δ_{F2} NMR parameters (*e.g.* R-VII and R-VIII). Thus, analysis of these NMR parameters is necessary to identify individual resonances in the spectrum. Comparison of the spectra of the hydrated Na-, Li-ZSM-5/A; Na-, H-ZSM-5/H; and Na-, Li-, H-ZSM-5/E (Table 2) indicates that there is no observable effect of the type of counter cation balancing the framework negative charge on the ^{27}Al NMR parameters of the hydrated ZSM-5 zeolite.

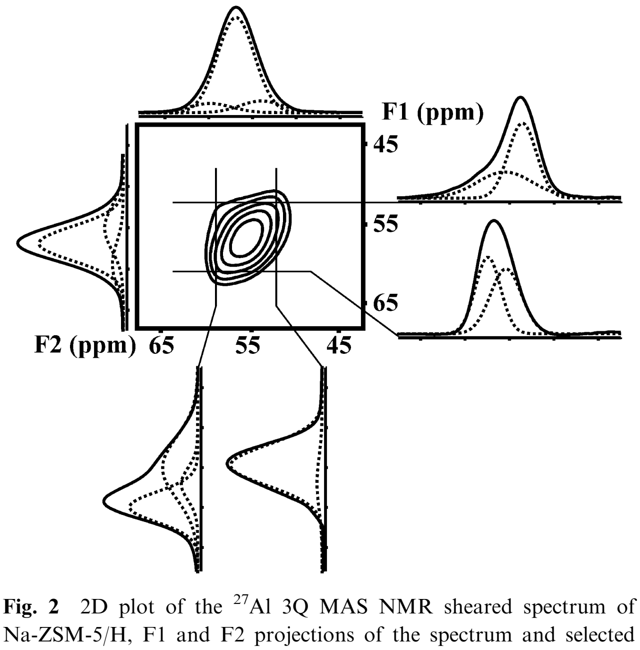

Fig. 2 2D plot of the ^{27}Al 3Q MAS NMR sheared spectrum of Na-ZSM-5/H, F1 and F2 projections of the spectrum and selected normalized slices and projection and slice simulations.

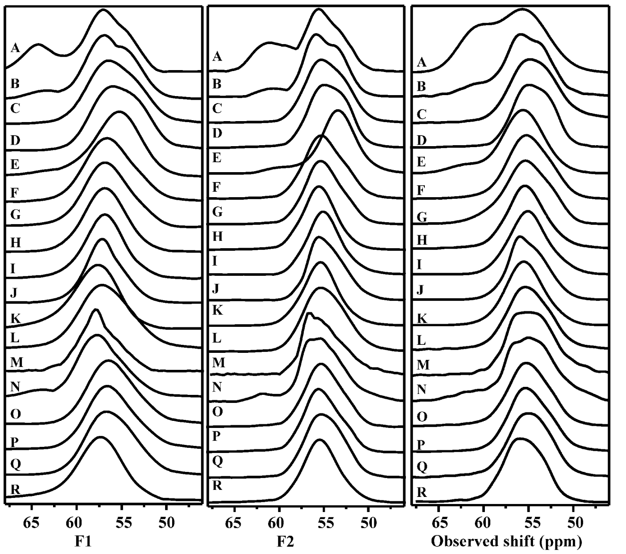

Fig. 3 F1 (left) and F2 (middle) projections of 2D ^{27}Al 3Q MAS NMR spectra and single pulse ^{27}Al MAS NMR spectra (right) for Na-ZSM-5/A-R zeolite samples.

Table 2 Effect of the counter cations on the ^{27}Al NMR parameters of the three resonances[a] of ZSM-5/A, ZSM-5/H, and ZSM-5/E zeolite samples determined from 3Q MAS NMR spectra

		ZSM-5/A		ZSM-5/H		ZSM-5/E		
	NMR Parameter	Counter cation						
Resonance[a]	(ppm)	Na	Li	Na	H	Na	Li	H
	δ_{F1}	54.6	54.3			54.9	55.0	54.8
III	δ_{F2}	52.5	52.6			52.3	52.3	52.4
	$\boldsymbol{\delta_{iso}}$	**53.8**	**53.7**			**53.9**	**54.0**	**53.9**
	δ_{F1}			55.1	55.0			
IV	δ_{F2}			53.6	53.4			
	$\boldsymbol{\delta_{iso}}$			**54.5**	**54.4**			
	δ_{F1}	56.9	57.1	56.9	56.8	57.1	57.2	57.2
VI	δ_{F2}	55.5	55.8	55.5	55.7	55.6	55.7	55.4
	$\boldsymbol{\delta_{iso}}$	**56.4**	**56.6**	**56.4**	**56.4**	**56.5**	**56.6**	**56.5**
	δ_{F1}			59.9	59.3			
IX	δ_{F2}			57.4	57.9			
	$\boldsymbol{\delta_{iso}}$			**59.0**	**58.8**			
	δ_{F1}	64.1	64.0					
XI	δ_{F2}	61.0	61.3					
	$\boldsymbol{\delta_{iso}}$	**62.9**	**63.0**					
	δ_{F1}					64.5	64.3	64.6
XII	δ_{F2}					62.0	62.4	61.7
	$\boldsymbol{\delta_{iso}}$					**63.6**	**63.6**	**63.5**

[a] See Table 3.

3.3 Al distribution in ZSM-5

At least 12 resonances, designated as I–XII, can be identified in the ^{27}Al 3Q MAS NMR spectra of the investigated Na-ZSM-5 zeolites (Table 3). Almost all resonances exhibit a low dispersion of the isotropic chemical shifts ($\leqq$0.2 ppm) and of the δ_{F1} and δ_{F2} values for the different ZSM-5 samples. This fact indicates that the accuracy of the estimation of the ^{27}Al NMR parameters is better than ±0.2 ppm for the majority of samples. Thus, each of the resonances I–V and VII–XII could be assigned to Al in one particular framework T-site. The scattered NMR parameters of the signal of R-VI

Table 3 NMR parameters of the individual resonances of the ZSM-5 samples A–R determined from ^{27}Al 3Q MAS NMR spectra

	A	B	C	D	E	F	G	H	I	J	K	L	M	N	O	P	Q	R	Average	Res.
Si/Al$_{FR}$	15	45	35	25	15	25	15	25	35	26	14	30	120	140	30	25	35	25	value	*Res*[a]
δ_{F1}			49.2	49.3		49.5													49.3 ± 0.1	I
δ_{F2}			51.1	51.2		51.3													51.2 ± 0.1	*I*
$\boldsymbol{\delta}_{\mathbf{iso}}$			**49.9**	**50.0**		**50.2**													**50.0 ± 0.1**	
δ_{F1}			53.2	53.3		53.3						53.0			53.3	53.3	53.4		53.3 ± 0.1	II
δ_{F2}			52.4	52.4		52.3						52.2			52.3	52.4	52.3		52.3 ± 0.1	*II*
$\boldsymbol{\delta}_{\mathbf{iso}}$			**52.9**	**53.0**		**52.9**						**52.7**			**52.9**	**53.0**	**53.0**		**52.9 ± 0.1**	
δ_{F1}	54.6	54.4			54.9		54.1				54.4		54.1	54.5					54.4 ± 0.3	III
δ_{F2}	52.5	52.5			52.3		52.5				52.4		52.5	52.4					52.4 ± 0.1	*III*
$\boldsymbol{\delta}_{\mathbf{iso}}$	**53.8**	**53.7**			**53.9**		**53.5**				**53.7**		**53.5**	**53.7**					**53.7 ± 0.1**	
δ_{F1}								55.1	55.4	55.5		55.2	55.2		55.1	55.2	55.2	55.2	55.2 ± 0.1	IV
δ_{F2}								53.6	53.6	53.6		53.2	53.3		53.8	53.9	53.6	53.7	53.6 ± 0.2	*IV*
$\boldsymbol{\delta}_{\mathbf{iso}}$								**54.5**	**54.7**	**54.8**		**54.5**	**54.5**		**54.6**	**54.7**	**54.6**	**54.6**	**54.6 ± 0.1**	
δ_{F1}									57.0				56.8	56.4					56.7 ± 0.2	V
δ_{F2}									54.9				54.9	54.8					54.9 ± 0.1	—
$\boldsymbol{\delta}_{\mathbf{iso}}$									**56.2**				**56.1**	**55.8**					**56.0 ± 0.2**	
δ_{F1}	56.9	56.9	56.7	57.4	57.1	56.8	57.1	56.9		57.4	57.6	57.2			56.7	56.8	56.7	57.1	57.0 ± 0.3	*VI*
δ_{F2}	55.5	55.4	55.3	55.7	55.6	55.3	55.4	55.5		55.4	55.3	55.5			55.4	55.5	55.6	55.4	55.4 ± 0.1	*V*
$\boldsymbol{\delta}_{\mathbf{iso}}$	**56.4**	**56.3**	**56.2**	**56.8**	**56.5**	**56.2**	**56.5**	**56.4**		**56.7**	**56.7**	**56.6**			**56.2**	**56.3**	**56.3**	**56.5**	**56.4 ± 0.2**	
δ_{F1}													58.6		58.5	58.7			58.6 ± 0.1	VII
δ_{F2}													56.9		57.7	57.4			57.3 ± 0.3	—
$\boldsymbol{\delta}_{\mathbf{iso}}$													**58.0**		**58.2**	**58.2**			**58.1 ± 0.1**	
δ_{F1}		59.2	59.0			59.0	59.5		59.0	59.3				59.3			59.0	59.3	59.2 ± 0.2	VIII
δ_{F2}		56.6	56.8			56.6	56.5		56.4	56.1				56.5			56.7	56.6	56.5 ± 0.2	*VI*
$\boldsymbol{\delta}_{\mathbf{iso}}$		**58.2**	**58.2**			**58.1**	**58.4**		**58.0**	**58.1**				**58.3**			**58.1**	**58.3**	**58.2 ± 0.1**	
δ_{F1}							60.0	59.9				59.7	59.6						59.8 ± 0.2	IX
δ_{F2}							57.3	57.4				57.3	57.6						57.4 ± 0.1	*VII*
$\boldsymbol{\delta}_{\mathbf{iso}}$							**59.0**	**59.0**				**58.8**	**58.9**						**58.9 ± 0.1**	
δ_{F1}											60.9			60.7					60.8 ± 0.1	X
δ_{F2}											58.5			58.7					58.6 ± 0.1	*VIII*
$\boldsymbol{\delta}_{\mathbf{iso}}$											**60.0**			**60.0**					**60.0 ± 0.1**	
δ_{F1}	64.1	63.9																	64.0 ± 0.1	XI
δ_{F2}	61.0	60.7																	60.9 ± 0.2	*IX*
$\boldsymbol{\delta}_{\mathbf{iso}}$	**63.0**	**62.7**																	**62.8 ± 0.1**	
δ_{F1}					64.5									64.4					64.5 ± 0.1	XII
δ_{F2}					62.0									61.8					61.9 ± 0.1	*X*
$\boldsymbol{\delta}_{\mathbf{iso}}$					**63.6**									**63.4**					**63.5 ± 0.1**	

[a] Notation of resonances in ref. 38.

can rather correspond to several unresolved resonances with very close shieldings but located at different T-sites. Note that each of the resonances I–XII was found for at least two samples. Moreover, the resonances III, IV, VI, IX, XI, and XII were also observed for the zeolites exchanged with different counter cations (Li$^+$, H$^+$). Thus, the attribution of the resolved resonances to an experimental artifact can be ruled out. At least two resonances of each sample were also observed for at least one more sample indicating that the change of the NMR parameters is not due to a variation of macroscopic parameters. We conclude that at least 12 framework T-sites are occupied by Al atoms in the set of the investigated ZSM-5 samples.

3.4 Quantification of Al distribution in ZSM-5

The details of the single pulse ^{27}Al MAS NMR spectra of the Na-zeolite samples in the tetrahedral region and their simulations are given in Fig. 3 and Fig. S2 of the ESI.† These spectra were used to quantify the concentration of the Al atoms in the individual T-sites. The estimated distribution of Al atoms is shown in Fig. 4. Both the siting as well as the relative concentration of Al in the individual T-sites vary significantly.

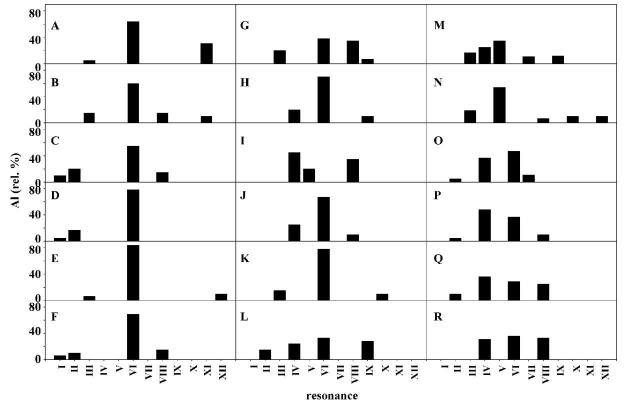

Fig. 4 Relative concentration of Al atoms of the resonances I–XII in the Na-ZSM-5/A-R zeolite samples.

4. Zeolite models used for calculations

High-resolution ^{27}Al MAS NMR spectra of zeolites can be successfully measured only for fully hydrated matrices due to the strong quadrupolar interaction of the aluminium atoms in dehydrated zeolite.[47] Thus, the NMR parameters characterizing the Al atoms and their environments in the ZSM-5 framework can be measured only for samples containing counter cations or H_3O^+ and water molecules. Due to the large number of possible configurations, isotropic chemical shift calculations including the hydration of zeolite and the solvated counter cation would require extensive sampling over isotropic chemical shifts calculated quantum mechanically for the individual configurations and structures.

To avoid this massive computational problem we look for a simple model of the complex structure of a hydrated zeolite. We adopt a bare charged framework with a single Al atom in a unit cell to describe the local geometry around the Al nucleus. This is a realistic model because of the reasons as follows: in completely hydrated zeolites, the fully solvated counter cation is located close to the center of the cavity/channel and does not directly interact with the AlO_4 tetrahedra as evidenced by a number of XRD studies of hydrated zeolites.[48] This fact is further supported, for example, by the optical spectroscopic studies of Co^{2+} or Cu^{2+} ions in hydrated zeolites.[49,50] Moreover, the cation in hydrated zeolites is rotationally free, as indicated by the sharp and narrow resonances in the ^{7}Li and ^{133}Cs MAS NMR spectra of hydrated Li-ZSM-5/E[51] and Cs-MOR,[52] respectively. Therefore, the effect of the hydrated counter cation on the local geometry of the AlO_4 tetrahedra in hydrated silicon rich zeolites and thus on the ^{27}Al isotropic chemical shift is negligible as shown in Table 2. This observation is in agreement with the result of Sarv *et al.* who reported a tiny difference 0–0.2 ppm in the F1 values of the resonances observed with Na- and Ca-ZSM-5.[22] Similar observations have been made on calculated ^{29}Si-NMR shifts for monosilicate species.[53] The calculated shifts for hydrated H^+ and K^+ counterions agree within 0.1 ppm.

The explanation of all these findings is that the shielding depends primarily on the local structure around the magnetic nucleus and that solvent and counterions do not affect the shielding by "through space" effects. Hence ^{27}Al isotropic chemical shift calculations can be made on models that do not include water molecules and counter ions explicitly. This assumption, by the way, is also implicit in the angle correlation model[25] that has been applied in previous studies.[23] Our model goes beyond it in as far as it includes up to five bonds away from the magnetic nucleus instead of two and it calculates the shieldings explicitly instead of relying on a correlation.

Table 4 Assignment of individual resonances of the ZSM-5 samples to T-sites based on calculated ^{27}Al NMR isotropic chemical shift parameters and resulting deviations (ppm)

	Assignment 1			Assignment 2		
Resonance	T-site	Shift	Deviation	T-site	Shift	Deviation
I	20	50.7	+0.7 ± 0.1	20	50.7	+0.7 ± 0.1
II	8	53.3	+0.4 ± 0.1	8	53.3	+0.4 ± 0.1
III	4	53.4	–0.3 ± 0.1	4	53.4	–0.3 ± 0.1
IV	6	55.1	+0.5 ± 0.1	6	55.1	+0.5 ± 0.1
X	7	60.0	0.0 ± 0.1	12	60.8	+0.8 ± 0.1
XI	17	62.5	–0.3 ± 0.1	1	63.7	+0.9 ± 0.1
XII	1	63.7	+0.2 ± 0.1	24	64.8	+1.3 ± 0.1
Range		13.0	–0.6		14.1	+0.5

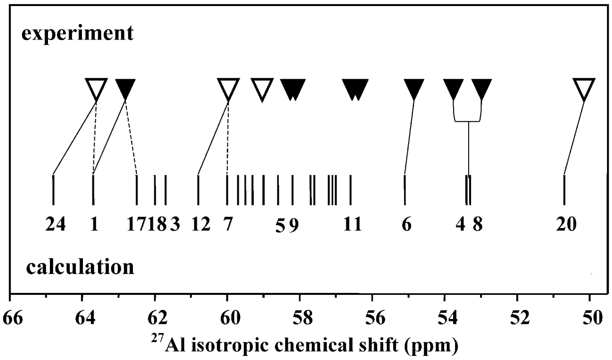

Fig. 5 Comparison of the theoretical and observed ^{27}Al isotropic chemical shifts in Na-ZSM-5 samples. Strong (▼) and weak (▽) resonances and Assignment 1 (– – –) and Assignment 2 (——).

We conclude that a bare charged framework with a single Al atom in a unit cell represents a realistic model to describe the Al local geometry and predict the ^{27}Al isotropic chemical shift for individual T-sites in ZSM-5. The final proof that this model is adequate can only come from a favorable agreement of calculated isotropic chemical shifts with observed ones. This is indeed the case as discussed in section 7.3. and exemplified by the close agreement between calculated (14.1) and measured (13.6 ppm) ranges of ^{27}Al isotropic chemical shifts (Table 4) and by the similar shift patterns (Fig. 5).

5. Computational methods

5.1 Models and optimization of structures

The computations are performed for a single Al atom in a unit cell of ZSM-5. A bare zeolite framework model is adopted that includes neither cations nor water molecules and possesses $P1$ symmetry. Each Al atom bears a formal charge of -1. The starting structure was generated from the X-ray structure of mutinaite,[54,55] which is the natural analogue of ZSM-5. First, both the lattice constants and the atomic positions of the all-silica MFI structure were optimized at constant pressure by the GULP program[56,57] using interatomic potential functions only. Then the silicon atom in the site of interest was replaced by an aluminium atom and the structure and the lattice constants were further optimized at constant pressure. The optimized structure was subsequently used for defining a cluster around the Al atom for our QM-Pot calculations.[39,40] The clusters were embedded into a super cell composed of two unit cells of the zeolite framework and the structure of the entire system was optimized by QMPOT at constant volume.

5.2 Cluster models

For all calculations, clusters having the Al atom in the center and including five coordination shells (Al–O–Si–O–Si–O–H_{link}) were used.[31] They were cut out from the corresponding optimized super cells. Due to the presence of silicate rings in the framework of ZSM-5, the created five-shell clusters contained pairs of very close H_{link} atoms. Since the close H_{link} atoms represented the same Si atom, they were replaced by the corresponding $Si(OH_{link})_2$ moiety. This was repeated until the cluster contained no such pairs.

5.3 QM-Pot method

The QM-Pot method employed[39,40] partitions the whole system (S) into two parts. The inner part (I) is treated by quantum mechanics (QM) and the outer part (O) as well as all the interactions between the inner and outer layers are treated by parametrized interatomic potential functions (Pot). The dangling bonds of the inner part are saturated by link hydrogen atoms. The atoms of the inner part together with the link atoms form the cluster (C). The QM-Pot energy of the whole system is given by

$$E^{\text{QM-Pot}}(\text{S}) = E^{\text{QM}}(\text{C}) + E^{\text{Pot}}(\text{S}) - E^{\text{Pot}}(\text{C})$$

where $E^{\text{QM}}(\text{C})$ is the energy of the cluster at the QM level, $E^{\text{Pot}}(\text{S})$ is the energy of the entire system at the Pot level and $E^{\text{Pot}}(\text{C})$ is the energy of the cluster at Pot. The QM-Pot approach is discussed in detail elsewhere.[58]

The calculations were performed by the QMPOT program[40] which utilizes the Turbomole program[59–63] for the QM part and the GULP program[56,57] for the periodic potential function calculations. The pure DFT method employing the BLYP[64–66] functional and the TZVP basis set of Ahlrichs[67] were used for the QM calculations. Shell-model ion-pair potentials[68] parametrized on DFT results for zeolites[69] were employed as interatomic potential functions (Pot). The electrostatic energy was evaluated by standard Ewald summation techniques for all cores and shells. A cut-off radius of 10 Å was chosen for the summation of short-range interactions.

5.4 Calculation of ^{27}Al isotropic chemical shifts

Subsequently to the QM-Pot structure determination, the Gaussian program[70] was employed to calculate NMR shielding tensors of the atoms of the optimized clusters at the BLYP/TZVP level using the gauge-independent atomic orbital method (GIAO).[30]

5.5 Conversion of chemical shieldings into ^{27}Al isotropic chemical shifts

A chabazite sample having a Si/Al ratio of 38 was employed to convert the calculated chemical shieldings into isotropic chemical shifts. A 2D plot of the ^{27}Al 3Q MAS NMR spectrum, F1 and F2 projections and their simulation of the sample are described in Fig. 6. Two resonances are present in the spectrum. The strong one exhibits an isotropic chemical shift at 60.0 ppm (F1 = 60.4 and F2 = 59.3), weak (*ca.* 25% of the intensity) resonance exhibits an isotropic chemical shift at 59.2 ppm (F1 = 60.0 and F2 = 57.9). The same approach and the same cluster size as described above were used to calculate the ^{27}Al chemical shielding of chabazite utilizing a model of four chabazite unit cells with one Al/Si substitution (Si/Al 47). The Al/Si substitution breaks down the symmetry of the chabazite framework and one distinguishable T-site of all-silica chabazite splits into three distinguishable T-sites. The QM-Pot relative energies, average T–O–T angles and ^{27}Al chemical shieldings of Al in the 3 T-sites of chabazite (Si/Al 47) are listed in Table 5. The differences between the distinguishable T-sites are significantly smaller than those for the ZSM-5 zeolite. The splitting of one T-site into 3 T-sites is reflected in three values of the calculated ^{27}Al chemical shielding, however, two of them have very similar values. This result is in very good agreement with the two observed ^{27}Al NMR resonances (Fig. 6) for the silicon rich chabazite. The ^{27}Al NMR shieldings of 490.0/489.9 and 490.4 ppm relate to the experimental values of 60.0 and 59.2 ppm, respectively, for the ^{27}Al isotropic chemical shift. The relation of the shielding of 490.0 corresponding to the ^{27}Al isotropic chemical shift of 60.0 ppm is used for the conversion of the calculated ^{27}Al NMR shieldings to ^{27}Al isotropic chemical shifts.

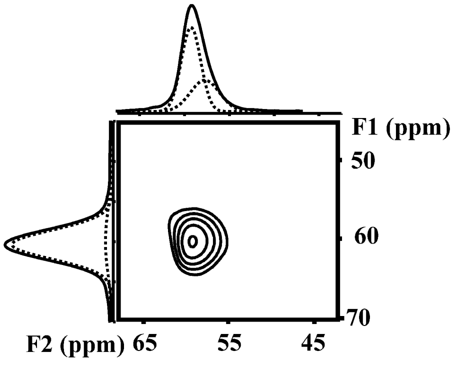

Fig. 6 2D plot of the ^{27}Al 3Q MAS NMR sheared spectrum of H-chabazite and F1 and F2 projections of the spectrum and their simulations.

Table 5 QM-Pot relative energies (kcal mol^{-1}), average T–O–T angles (°) and ^{27}Al chemical shieldings (ppm) of Al in the 3 T-sites of chabazite (Si/Al 47)

Site			
T1[a]	0.0	145.4	490.4
T2	1.6	145.6	490.0
T3	3.4	144.7	489.9

[a] The Cartesian coordinates with T-site designations are shown in the ESI.

6. Local AlO_4 structures and ^{27}Al NMR shieldings

Our QM-Pot calculations of ZSM-5 structures (*P*1 symmetry) containing one Al atom per unit cell resulted in 24 distinguishable structures corresponding to Al substitution into the 24 T-sites of monoclinic ZSM-5. The force field relative energies of Al in the 24 T-sites of ZSM-5 are all within 10 kcal mol^{-1} (Table S2 of the ESI†). This is similar to previous studies.[11,15] The sites T13 and T5 are most stable, T18 is the least stable site.

Table 6 shows the calculated average T–O–T angles, the GIAO ^{27}Al NMR shieldings and the corresponding isotropic chemical shifts (calibrated employing the chabazite zeolite, see section 5.5) for the 24 T-sites; for the four individual T–O–T angles of each site see Table S3 of the ESI.† The calculated Al–O–Si angles scatter between 124 and 172°, but the average Al–O–Si angles vary significantly less—from 140° (T24 site) to 154° (T20 site). The site with the smallest average angle (T24) corresponds to the smallest GIAO-calculated ^{27}Al NMR shielding, 485.2 ppm, and the one with the largest average angle (T20 site) to the largest shielding, 499.3 ppm. Note that a higher shielding corresponds to a lower isotropic chemical shift.

Table 6 BLYP GIAO ^{27}Al NMR shieldings (ppm) and isotropic chemical shifts^{a} (ppm) and average Al–O–Si angles (°) for the individual T-sites of ZSM-5

T-site	Shielding	Shift	Al–O–Si
1	486.3	63.7	143.5
2	492.9	57.1	144.8
3	488.3	61.7	140.3
4	496.6	53.4	151.4
5	491.4	58.6	144.7
6	494.9	55.1	150.5
7	490.0	60.0	143.3
8	496.7	53.3	149.1
9	491.8	58.2	144.3
10	492.3	57.7	146.1
11	493.3	56.7	146.6
12	489.2	60.8	143.2
13	490.3	59.7	144.4
14	490.7	59.3	142.4
15	492.4	57.6	153.5
16	492.9	57.1	144.0
17	487.5	62.5	140.8
18	488.0	62.0	145.2
19	490.5	59.5	142.5
20	499.3	50.7	154.3
21	493.0	57.0	148.2
22	491.0	59.0	141.9
23	492.8	57.2	145.8
24	485.2	64.8	139.8

[a] The ^{27}Al NMR isotropic chemical shifts were obtained by conversion of the BLYP GIAO shieldings using the calculated and measured shielding/shift values of 490.0 and 60.0 ppm, respectively, for the chabazite sample (Si/Al 38), see section 5.4.

Based on comparison between the crystallographic and ^{27}Al NMR data of aluminium rich zeolites, Lippmaa *et al.*[25] suggested a linear correlation between the ^{27}Al NMR isotropic chemical shift δ(Al) and the average T–O–T angle (θ) of the zeolite framework.

$$\delta(\mathrm{Al}) = -0.50\theta + 132 \text{ ppm}$$

The calculated GIAO ^{27}Al NMR isotropic chemical shifts are plotted against the average Al–O–Si angles in Fig. 7. The plot shows that the linear correlation does not hold even when the calculated Al–O–Si angles are used instead of crystallographic T–O–T angles. Let us select two pairs of sites from Table 6 (see also Fig. 7) to illustrate this point. The average Al–O–Si angles for T1 and T7 are virtually identical (143.5 and 143.3°, respectively). Thus the isotropic chemical shifts δ(Al) calculated using linear correlation were essentially the same, whereas the GIAO ^{27}Al NMR isotropic chemical shifts vary significantly (63.7 and 60.0 ppm, respectively). On the contrary, the T10 and T15 sites differ considerably in their average T–O–T angles (146.1 and 153.5°, respectively) but their GIAO ^{27}Al NMR isotropic chemical shifts differ by 0.1 ppm only (57.7 and 57.6 ppm, respectively). These examples show that there is no simple linear correlation between the ^{27}Al NMR isotropic chemical shift and the corresponding average T–O–T angle of the AlO_4 tetrahedron.

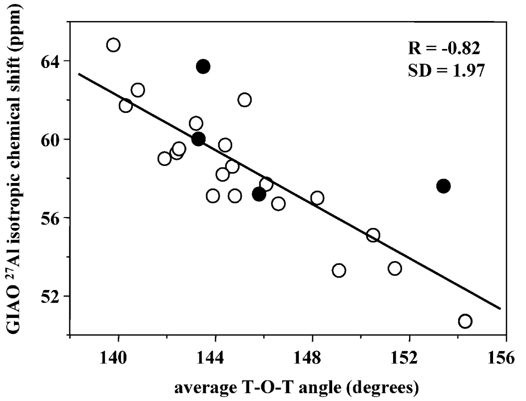

Fig. 7 GIAO ^{27}Al isotropic chemical shifts plotted against the average T–O–T angles for the 24 T-sites of ZSM-5. (●) indicates T1 and T7 as well as T10 and T15 pairs.

Our conclusion regarding the failure of the linear correlation is in agreement with that reached by Kučera and Nachtigal[37] for the MCM-58 zeolite from periodic DFT results. They explained the failure by different effects of the Na^+ counter cation and its hydration degree on the geometry of the four distinguishable T-sites. On the contrary, our results clearly indicate that the relationship between the ^{27}Al NMR isotropic chemical shift and the local geometry of AlO_4 is more complex and does not depend only on the average Al–O–Si angles.

7. Discussion

7.1 Al siting in ZSM-5

As detailed in the Results section, the observed resonances for all ZSM-5 samples correspond to Al located in at least 12 different tetrahedral sites of the zeolite framework. Two new resonances were identified compared to our preliminary results reported in ref. 38 This can be explained by a significantly larger set of ZSM-5 samples used. The local coordination of Al and its isotropic chemical shift could be affected by the atom type (Si or Al) of the second neighboring T-sites of the Al atom. Thus, the assignment of several observed Al resonances to one framework T-site cannot be excluded *a priori*. The Si/Al ratios of the ZSM-5 samples considered are in the 14–140 interval. Our ^{29}Si NMR measurements show that there are no Al–O–Si–O–Al pairs, which allows us to rule out the effect of an Al atom as a next-nearest neighbor. There is also a low population of close Al atoms (Al–O–(Si–O)$_2$–Al sequences) in the samples as our cobalt(II) exchange experiments indicate. Moreover, no correlation between the presence of the close Al atoms and the observed ^{27}Al resonances was found. Thus the 12 observed resonances correspond to Al atoms in 12 distinguishable framework T-sites indicating that at least half of the 24 distinguishable T-sites predicted by our QM-Pot calculations are occupied in the set of the investigated ZSM-5 samples.

A previous study,[23] in which only two resonances have been resolved, came to a different conclusion. The authors employed the empirical isotropic chemical shift—average T–O–T angle correlation[25] to predict ^{27}Al NMR isotropic chemical shifts from the (orthorhombic) XRD structure of a ZSM-5 sample with an Si/Al ratio of 86. The calculated isotropic chemical shifts for the 12 T-sites varied over a range of 5.1 ppm only. Furthermore, all the F1 and F2 parameters calculated for the 12 T-sites fell into the observed 3Q spectrum.[23] The present calculations show that this is an artifact due to the use of the bond angles from the X-ray structure. These are essentially Si–O–Si bond angles with only small contributions of Si–O–Al bond angles because of the low Al content.

The 12 resonances identified in the spectra of Na-ZSM-5 samples represent a significant progress compared to previous studies.[22,23] Sarv *et al.*[22] could report only three Al resonances, which is due to the fact that they examined just one ZSM-5 sample. Also in the present study there are only between three and five T-sites occupied by Al in a given ZSM-5 sample, but there are 18 different samples. Han *et al.*[23] report only two resonances. They investigated a set of samples, all prepared by one procedure and differing only in the framework Al concentration. In addition, the structure-directing agent was not removed from their samples.

Note that the isotropic chemical shifts reported by Sarv[22] (54.5, 57.1 and 59.4 ppm) are close to the resonances IV, VI and IX which we find at 54.6, 56.4 and 58.9 ppm, but a safe assignment cannot be made, for the sample investigated by Sarv *et al.*[22] was not examined for the presence of Al–O–(Si–O)$_2$–Al sequences which can affect the Al isotropic chemical shift.

7.2 Al distribution over T-sites of the ZSM-5 framework

The results shown in Table 3 and Fig. 4 clearly indicate a large variability in both sites occupied by Al atoms and the concentration of the Al atoms in these sites for the ZSM-5 samples studied. Even samples with similar framework aluminium concentration exhibit very different Al sitings as well as Al concentrations in the individual occupied T-sites. This fact clearly rules out that the Al siting in the zeolite framework is random or is controlled by thermodynamic stability. It rather shows that the conditions of the synthesis are responsible for the Al siting in the framework. A similar conclusion was reached based on the presence of Al–O–(Si–O)$_{1,2}$–Al sequencies and isolated Al atoms (Al–O–(Si–O)$_{n>2}$–Al) in ZSM-5 zeolites.[45,46,71] Corma *et al.* discussed the role of the structure directing agents[72,73] or fluorine anions[74] on the Al siting in zeolites.

The observed non-random Al siting in ZSM-5 is in good agreement with the results of the high-resolution ^{27}Al NMR experiments not only for ZSM-5,[22,23] but also for the zeolite Beta.[75] This shows that the dependence of the Al siting on the synthesis conditions may be a general feature of silicon-rich zeolites.

Our results summarized in Fig. 4 point to a complex relationship between the conditions of the zeolite syntheses and the Al siting, but one observation regarding the Al distribution is made. The site corresponding to R-VI is significantly more often occupied in the investigated samples than the other ones. However, the high occupation is likely caused by the fact that this resonance represents several T-sites having close NMR parameters as Fig. 5 shows.

Fig. 8 shows the effect of Si/Al on the number of T-sites occupied by Al atoms. Clearly, there is no effect of the framework Al content on the number of occupied T-sites. From three to five T-sites are occupied by Al in the whole concentration range (Si/Al 14–140). This conclusion is counterintuitive and indicates that the conditions and mechanisms of the zeolite synthesis are crucial for the Al distribution in the zeolite framework.

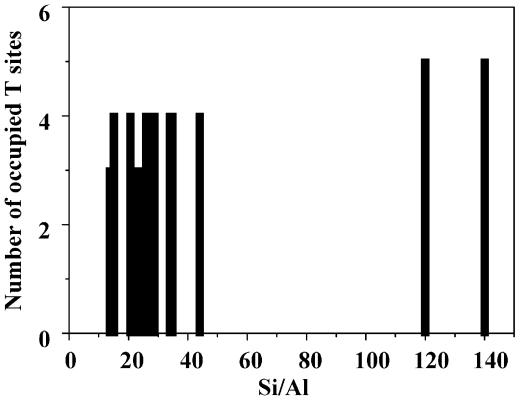

Fig. 8 Number of T-sites occupied by Al atoms in the ZSM-5 samples plotted against their Si/Al ratio.

7.3 Assignment of observed resonances to T-sites

Fig. 5 compares the calculated and measured ^{27}Al isotropic chemical shifts. The values for the different T-sites extend over the ranges of 14.1 and 13.6 ppm, respectively. In addition, the patterns of the predicted and observed isotropic chemical shifts show similarities. Based on similar spacings and least deviations between calculated and observed isotropic chemical shifts a partial assignment of observed resonances to crystallographic sites in ZSM-5 is possible (Table 4): Resonance I (hereafter R-I) corresponds to T20 and R-IV to T6. The pair R-II, R-III can be assigned to the T4, T8 pair. At the low-shielding end, two assignments are plausible. The smallest deviations between the calculated and observed isotropic chemical shifts are reached if it is assumed that T24 (64.8 ppm) is not occupied in the samples and that R-XII belongs to T1, R-XI to T17 and R-X to T7. The isotropic chemical shift deviations are all between +0.7 and −0.3 ppm and the calculated range is 13.0 ppm, 0.6 ppm smaller than the I to XII range of observed resonances (13.6 ppm). It follows then that T-sites T12 (60.8), T3 (61.7), and T18 (62.0) are most likely not occupied by Al in our ZSM-5 samples. To which of the remaining 13 T-sites Resonances V to IX belong remains open, see Fig. 5. If we assume that the calculated isotropic chemical shifts are systematically larger than the observed ones by 0.7–1.3 ppm (see Fig. 5 and Table 3) due to a shift of the secondary standard we can assign R-XII and R-XI with the largest isotropic chemical shifts to the least shielded T24 and T1 sites, respectively, and R-X to T12. Then the sites T3 (61.7), T18 (62.0), and T17 (62.5) would be unoccupied by Al in our ZSM-5 samples. This second assignment leads to deviations between +1.3 and –0.3 ppm and the calculated isotropic chemical shift range (14.1 ppm) would be 0.5 ppm larger than the observed one.

These results represent a significant progress in interpreting ^{27}Al MAS NMR spectra of zeolites and the first partially successful analysis of the Al siting in a framework of a silicon-rich zeolite. These achievements clearly demonstrate the power of the high resolution NMR experiment combined with DFT (QM-Pot) calculations and also support the pure framework model adopted in the calculations. The chosen experimental approach of controlling the Al siting in silicon-rich zeolites by varying the synthesis conditions can be employed to investigate the effect of the Al siting on the physicochemical properties of zeolite catalysts. This might lead to a better design of acidic and redox catalysts with a controlled Al siting and thus tuned properties of the active sites.

8. Conclusions

In this paper, we have demonstrated that a combined experimental (^{27}Al 3Q MAS NMR) and theoretical (QM-Pot employing the bare framework model) approach represents a powerful tool for the determination of the local geometry of framework AlO_4 tetrahedra, the prediction of ^{27}Al isotropic chemical shifts in hydrated zeolites, and the identification of Al siting in the framework of silicon-rich zeolites.

Experimental evidence is provided for the occupation of at least 12 out of 24 distinguishable framework T-sites by Al atoms in silicon-rich ZSM-5. The observed ^{27}Al isotropic chemical shifts of 50.0 and 54.7 correspond to Al atoms in the T20 and T6 sites, respectively. The pair of resonances at 52.9 and 53.7 ppm corresponds to the pair of the T8 and T4 sites. At the low-shielding end, two assignments are plausible. The smallest deviations between the calculated and observed isotropic chemical shifts are reached if it is assumed that T24 (64.8 ppm) is not occupied in the samples and that R-XII belongs to T1, R-XI to T17 and R-X to T7. It follows then that T-sites T12 (60.8), T3 (61.7), and T18 (62.0) are most likely not occupied by Al in our ZSM-5 samples. If we assume that the calculated isotropic chemical shifts are systematically larger than the observed ones then we can assign R-XII and R-XI with the largest isotropic chemical shifts to the least shielded T24 and T1 sites, respectively, and R-X to T12. Then the sites T3 (61.7), T18 (62.0), and T17 (62.5) would be unoccupied by Al in our ZSM-5 samples. The assignment of the remaining three resonances remains ambiguous. The conclusion is reached that the Al distribution over framework T-sites is neither random nor controlled by a simple rule, but depends on the conditions of zeolite synthesis.

Furthermore, although there is a trend for smaller ^{27}Al isotropic chemical shifts with increasing average Al–O–Si bond angles, we have shown that the correlation is not good enough for assignment purposes. Therefore, the local geometry of framework AlO_4 tetrahedra cannot be inferred from experimental isotropic chemical shifts but can only be obtained from theoretical calculations.

Acknowledgements

This work was financially supported by the Academy of Sciences of the Czech Republic (project # 1ET400400413), the Grant Agency of the Czech Republic (project # 203/06/1449), Center of Excellence IDECAT NMP3-CT-2005-011730, and by the German Science Foundation (DFG) and the Funds of the German Chemical Industry (FCI). We would also like to thank Prof. Peter F. Rogl of the University of Vienna, Austria for helpful discussions on crystallography questions. We would also like to thank Dr Qingjun Zhu of Tokyo Institute of Technology, Japan for providing us a sample of the silicon rich chabazite.

References

1 C. D. Chang, *Catal. Rev. Sci. Eng.*, 1983, **25**, 1–118.
2 A. Corma and A. Martinez, *Catal. Rev. Sci. Eng.*, 1993, **35**, 483–570.
3 G. Bellussi, G. Pazzuconi, C. Perego, G. Girotti and G. Terzoni, *J. Catal.*, 1995, **157**, 227–234.
4 J. Cejka and B. Wichterlova, *Catal. Rev. Sci. Eng.*, 2002, **44**, 375–421.
5 M. Shelef, *Chem. Rev.*, 1995, **95**, 209–225.
6 H. Yahiro and M. Iwamoto, *Appl. Catal., A*, 2001, **222**, 163–181.
7 G. I. Panov, A. S. Kharitonov and V. I. Sobolev, *Appl. Catal., A*, 1993, **98**, 1–20.
8 S. M. Csicsery, *Pure Appl. Chem.*, 1986, **58**, 841–856.
9 J. N. Armor, *Microporous Mesoporous Mater.*, 1998, **22**, 451–456.
10 B. Wichtelova, Z. Sobalik and J. Dedecek, *Appl. Catal., B*, 2003, **41**, 97–114.
11 K. P. Schroder, J. C. Sauer, M. Leslie, C. Richard and A. Catlow, *Zeolites*, 1992, **12**, 20–23.
12 S. R. Lonsinger, A. K. Chakraborty, D. N. Theodorou and A. T. Bell, *Catal. Lett.*, 1991, **11**, 209–217.
13 F. Blanco, G. Urbinavillalba and M. M. R. Deagudelo, *Mol. Simul.*, 1995, **14**, 165–176.
14 R. Grau-Crespo, A. G. Peralta, A. R. Ruiz-Salvador, A. Gomez and R. Lopez-Cordero, *Phys. Chem. Chem. Phys.*, 2000, **2**, 5716–5722.
15 D. Nachtigallova, P. Nachtigall, M. Sierka and J. Sauer, *Phys. Chem. Chem. Phys.*, 1999, **1**, 2019–2026.
16 A. E. Alvaradoswaisgood, M. K. Barr, P. J. Hay and A. Redondo, *J. Phys. Chem.*, 1991, **95**, 10031–10036.
17 D. H. Olson, N. Khosrovani, A. W. Peters and B. H. Toby, *J. Phys. Chem. B*, 2000, **104**, 4844–4848.
18 G. Engelhardt, B. Fahlke, M. Magi and E. Lippmaa, *Z. Phys. Chem. (Leipzig)*, 1985, **266**, 239–245.
19 J. Klinowski, J. M. Thomas, C. A. Fyfe, G. C. Gobbi and J. S. Hartman, *Inorg. Chem.*, 1983, **22**, 63–66.
20 C. A. Fyfe, G. C. Gobbi, J. Klinowski, A. Putnis and J. M. Thomas, *J. Chem. Soc., Chem. Commun.*, 1983, 556–558.
21 L. B. Alemany, *Appl. Magn. Reson.*, 1993, **4**, 179–201.
22 P. Sarv, C. Fernandez, J. P. Amoureux and K. Keskinen, *J. Phys. Chem.*, 1996, **100**, 19223–19226.
23 O. H. Han, C. S. Kim and S. B. Hong, *Angew. Chem., Int. Ed.*, 2002, **41**, 469–472.
24 J. A. van Bokhoven, D. C. Koningsberger, P. Kunkeler, H. van Bekkum and A. P. M. Kentgens, *J. Am. Chem. Soc.*, 2000, **122**, 12842–12847.
25 E. Lippmaa, A. Samoson and M. Magi, *J. Am. Chem. Soc.*, 1986, **108**, 1730–1735.
26 G. Engelhardt and R. Radeglia, *Chem. Phys. Lett.*, 1984, **108**, 271–274.
27 S. L. Lawton, A. S. Fung, G. J. Kennedy, L. B. Alemany, C. D. Chang, G. H. Hatzikos, D. N. Lissy, M. K. Rubin, H. K. C. Timken, S. Steuernagel and D. E. Woessner, *J. Phys. Chem.*, 1996, **100**, 3788–3798.
28 G. J. Kennedy, S. L. Lawton, A. S. Fung, M. K. Rubin and S. Steuernagel, *Catal. Today*, 1999, **49**, 385–399.
29 M. Derewinski, P. Sarv and A. Mifsud, *Catal. Today*, 2006, **114**, 197–204.
30 K. Wolinski, J. F. Hinton and P. Pulay, *J. Am. Chem. Soc.*, 1990, **112**, 8251–8260.
31 B. Bussemer, K. P. Schroder and J. Sauer, *Solid State Nucl. Magn. Reson.*, 1997, **9**, 155–164.
32 K. P. Schroder and J. Sauer, *J. Phys. Chem.*, 1996, **100**, 11043–11049.
33 L. M. Bull, B. Bussemer, T. Anupold, A. Reinhold, A. Samoson, J. Sauer, A. K. Cheetham and R. Dupree, *J. Am. Chem. Soc.*, 2000, **122**, 4948–4958.

34 L. M. Bull, A. K. Cheetham, T. Anupold, A. Reinhold, A. Samoson, J. Sauer, B. Bussemer, Y. Lee, S. Gann, J. Shore, A. Pines and R. Dupree, *J. Am. Chem. Soc.*, 1998, **120**, 3510–3511.
35 M. Profeta, F. Mauri and C. J. Pickard, *J. Am. Chem. Soc.*, 2003, **125**, 541–548.
36 P. Nachtigall and J. Sauer, in *Introduction to Zeolite Molecular Sieves*, ed. H. van Bekkum, J. Cejka, A. Corma, F. Schueth, (Stud. in *Surf. Sci. Catal.*, 168) Elsevier, Amsterdam, 2007, pp. 701–736.
37 J. Kucera and P. Nachtigall, *Microporous Mesoporous Mater.*, 2005, **85**, 279–283.
38 For a preliminary report, see S. Sklenak, J. Dedecek, C. B. Li, B. Wichterlova, V. Gabova, M. Sierka and J. Sauer, *Angew. Chem., Int. Ed.*, 2007, **46**, 7286–7289.
39 U. Eichler, C. M. Kolmel and J. Sauer, *J. Comput. Chem.*, 1997, **18**, 463–477.
40 M. Sierka and J. Sauer, *J. Chem. Phys.*, 2000, **112**, 6983–6996.
41 Q. Zhu, J. N. Kondo, T. Tatsumi, S. Inagaki, R. Ohnuma, Y. Kubota, Y. Shimodaira, H. Kobayashi and K. Domen, *J. Phys. Chem. C*, 2007, **111**, 5409–5415.
42 C. A. Fyfe, G. C. Gobbi and G. J. Kennedy, *J. Phys. Chem.*, 1984, **88**, 3248–3253.
43 J. M. Thomas and J. Klinowski, *Adv. Catal.*, 1985, **33**, 199–374.
44 G. Engelhardt, U. Lohse, E. Lippmaa, M. Tarmak and M. Magi, *Z. Anorg. Allg. Chem.*, 1981, **482**, 49–64.
45 J. Dedecek, D. Kaucky, B. Wichterlova and O. Gonsiorova, *Phys. Chem. Chem. Phys.*, 2002, **4**, 5406–5413.
46 J. Dedecek, D. Kaucky and B. Wichterlova, *Chem. Commun.*, 2001, 970–971.
47 J. Jiao, J. Kanellopoulos, W. Wang, S. S. Ray, H. Foerster, D. Freude and M. Hunger, *Phys. Chem. Chem. Phys.*, 2005, **7**, 3221–3226.
48 W. J. Mortier, *Zeolites*, 1982, 1–67.
49 J. Dedecek and B. Wichterlova, *J. Phys. Chem. B*, 1999, **103**, 1462–1476.
50 J. Dedecek and B. Wichterlova, *J. Phys. Chem. B*, 1997, **101**, 10233–10240.
51 J. Dedecek, Unpublished results.
52 P. J. Chu, B. C. Gerstein, J. Nunan and K. Klier, *J. Phys. Chem.*, 1987, **91**, 3588–3592.
53 V. Moravetski, J. R. Hill, U. Eichler, A. K. Cheetham and J. Sauer, *J. Am. Chem. Soc.*, 1996, **118**, 13015–13020.
54 E. Galli, G. Vezzalini, S. Quartieri, A. Alberti and M. Franzini, *Zeolites*, 1997, **19**, 318–322.
55 G. Vezzalini, S. Quartieri, E. Galli, A. Alberti, G. Cruciani and A. Kvick, *Zeolites*, 1997, **19**, 323–325.
56 J. D. Gale, *J. Chem. Soc., Faraday Trans.*, 1997, **93**, 629–637.
57 J. D. Gale and A. L. Rohl, *Mol. Simul.*, 2003, **29**, 291–341.
58 M. Brandle and J. Sauer, *J. Am. Chem. Soc.*, 1998, **120**, 1556–1570.
59 K. Eichkorn, F. Weigend, O. Treutler and R. Ahlrichs, *Theor. Chem. Acc.*, 1997, **97**, 119–124.
60 K. Eichkorn, O. Treutler, H. Ohm, M. Haser and R. Ahlrichs, *Chem. Phys. Lett.*, 1995, **242**, 652–660.
61 K. Eichkorn, O. Treutler, H. Ohm, M. Haser and R. Ahlrichs, *Chem. Phys. Lett.*, 1995, **240**, 283–289.
62 O. Treutler and R. Ahlrichs, *J. Chem. Phys.*, 1995, **102**, 346–354.
63 M. Haser and R. Ahlrichs, *J. Comput. Chem.*, 1989, **10**, 104–111.
64 B. Miehlich, A. Savin, H. Stoll and H. Preuss, *Chem. Phys. Lett.*, 1989, **157**, 200–206.
65 A. D. Becke, *Phys. Rev. A*, 1988, **38**, 3098–3100.
66 C. T. Lee, W. T. Yang and R. G. Parr, *Phys. Rev. B: Condens. Matter Mater. Phys.*, 1988, **37**, 785–789.
67 A. Schafer, C. Huber and R. Ahlrichs, *J. Chem. Phys.*, 1994, **100**, 5829–5835.
68 C. R. A. Catlow, M. Dixon and W. C. Mackrodt, *Lect. Notes Phys.*, 1982, **166**, 130–161.
69 M. Sierka and J. Sauer, *Faraday Discuss.*, 1997, **106**, 41–62.
70 M. J. Frisch, G. W. Trucks, H. B. Schlegel, G. E. Scuseria, M. A. Robb, J. R. Cheeseman, J. A. Montgomery, Jr., T. Vreven, K. N. Kudin, J. C. Burant, J. M. Millam, S. S. Iyengar, J. Tomasi, V. Barone, B. Mennucci, M. Cossi, G. Scalmani, N. Rega, G. A. Petersson, H. Nakatsuji, M. Hada, M. Ehara, K. Toyota, R. Fukuda, J. Hasegawa, M. Ishida, T. Nakajima, Y. Honda, O. Kitao, H. Nakai, M. Klene, X. Li, J. E. Knox, H. P. Hratchian, J. B. Cross, V. Bakken, C. Adamo, J. Jaramillo, R. Gomperts, R. E. Stratmann, O. Yazyev, A. J. Austin, R. Cammi, C. Pomelli, J. Ochterski, P. Y. Ayala, K. Morokuma, G. A. Voth, P. Salvador, J. J. Dannenberg, V. G. Zakrzewski, S. Dapprich, A. D. Daniels, M. C. Strain, O. Farkas, D. K. Malick, A. D. Rabuck, K. Raghavachari, J. B. Foresman, J. V. Ortiz, Q. Cui, A. G. Baboul, S. Clifford, J. Cioslowski, B. B. Stefanov, G. Liu, A. Liashenko, P. Piskorz, I. Komaromi, R. L. Martin, D. J. Fox, T. Keith, M. A. Al-Laham, C. Y. Peng, A. Nanayakkara, M. Challacombe, P. M. W. Gill, B. G. Johnson, W. Chen, M. W. Wong, C. Gonzalez and J. A. Pople, *GAUSSIAN 03 (Revision C.02)*, Gaussian, Inc., Wallingford, CT, 2004.
71 V. Gabova, J. Dedecek and J. Cejka, *Chem. Commun.*, 2003, 1196–1197.
72 G. Sastre, S. Leiva, M. J. Sabater, I. Gimenez, F. Rey, S. Valencia and A. Corma, *J. Phys. Chem. B*, 2003, **107**, 5432–5440.
73 G. Sastre, V. Fornes and A. Corma, *J. Phys. Chem. B*, 2002, **106**, 701–708.
74 M. A. Camblor, A. Corma and S. Valencia, *J. Mater. Chem.*, 1998, **8**, 2137–2145.
75 A. Abraham, S. H. Lee, C. H. Shin, S. B. Hong, R. Prins and J. A. van Bokhoven, *Phys. Chem. Chem. Phys.*, 2004, **6**, 3031–3036.